

Structure of LPCVD Tungsten Films for IC Applications

T. I. Kamins,* D. R. Bradbury,* T. R. Cass, S. S. Laderman, and G. A. Reid

Hewlett-Packard Laboratories, Palo Alto, California 94303-0867

ABSTRACT

Because of the widespread potential use of CVD tungsten films in integrated circuit applications, the structural properties of these films were examined over a range of deposition conditions and with different nucleating layers. When tungsten is deposited on a chromium nucleating layer on an oxidized silicon wafer, the stress is not a strong function of film thickness, and most of it is caused by the difference in the thermal coefficients of expansion of tungsten and silicon. The surface roughness increases almost linearly with increasing film thickness. The grain size also increases with increasing film thickness, with the diameters of the largest grains comparable to the film thickness. The structure is equiaxed, rather than columnar. The (100) texture is dominant near the normal deposition temperature of 300°C for different film thicknesses and nucleating layers, but the dominant orientation changes at higher deposition temperatures. The structure develops as the film is deposited, rather than being determined by the nucleation.

As the dimensions of integrated-circuit features continue to decrease, the potential use of chemically vapor-deposited tungsten films in the metalization system becomes increasingly attractive for many IC applications (1, 2). The resistivity of tungsten is much lower than that of polysilicon (although somewhat higher than that of aluminum), and tungsten is resistant to electromigration. It does not interact with silicon at moderate temperatures (3), so it can be used to make direct contact to the silicon electrodes of a device. Selective deposition can be used to preferentially deposit tungsten in contact holes to serve as a diffusion barrier and can also provide an etch stop during fabrication. If thick enough, it can fill contact holes between a metal line and silicon or vias to a lower level of metalization to provide a more planar surface. It can also be used to deposit metal selectively over the source, gate, and drain regions of MOS transistors.

To allow development of a stable, reproducible process for the deposition of CVD tungsten films, information is needed about the film properties and the sensitivity of these properties to variations in the deposition parameters. For example, the resistivity of the film is critical when the tungsten is used for long conducting lines; the structure is important for barrier applications. The deposition process selected should minimize the sensitivity of the film properties to variations in the deposition parameters.

The dependence of the selective deposition on the insulating layers exposed to the process gases during deposition and the interaction of silicon and tungsten after deposition have been previously reported (4, 3). In this paper, structural properties of deposited films are considered in more detail over a range of deposition conditions. To separate the effects of the initial silicon-reduction reaction, which occurs when tungsten is deposited directly on silicon, from those of the subsequent hydrogen reduction reaction, many of the films were deposited on chromium nucleating layers on oxidized silicon wafers. The variation of the film properties with increasing film thickness was examined in the greatest detail. The surface roughness, the stress, and the development of the structure with increasing film thickness were investigated. The characteristics of the films were also studied as the deposition temperature was varied from 250° to 375°C. Other nucleating layers, including lightly doped and heavily doped single-crystal and polycrystalline silicon, were also investigated. Although the deposition parameters were selected to be consistent with selective tungsten deposition, the material characteristics found should be relevant to tungsten films formed by either selective or nonselective processes.

Film Deposition

Tungsten films were deposited in a tube-type LPCVD reactor using WF_6 and hydrogen. The deposition kinetics were studied and found to be similar to those reported by Broadbent and Ramiller (5). Most films were depos-

ited at a temperature of 300°C with a WF_6 flow of 7 cm^3/min and an $H_2:WF_6$ ratio of 20:1. The total pressure was 0.26 torr (35 Pa). The deposition rate under these conditions was about 3 nm/min, and the deposition time was varied to obtain the desired film thickness. In some experiments, the temperature was varied over the range 250°-375°C with the gas flows kept constant.

To minimize the influence of the underlying substrate on the film properties, most films were deposited on thin layers of chromium sputtered onto lightly doped, single-crystal, silicon wafers oxidized at 1000°C in a TCA/ O_2 ambient. The chromium layer was nominally about 8 nm thick and promoted both nucleation of the tungsten and adhesion of the film to the oxide surface. The effect of the underlying substrate on the film structure was also considered by depositing tungsten films on single-crystal silicon wafers and on wafers covered with one of a number of different nucleating layers. Before the wafers were loaded into the reactor, those with thicker nucleating layers were etched in 10:1 $H_2O:HF$ for 15-20s to clean the surface. Wafers with very thin nucleating layers were not cleaned between formation of the nucleating layer and tungsten deposition.

The sheet resistance was measured with a four-point probe and was uniform over the sample within better than 5% for all except the very thinnest films. The resistivity was 13.9 $\mu\Omega\text{-cm}$ for films about 162 nm thick and decreased to 10.5 $\mu\Omega\text{-cm}$ for films about 430 nm thick, in reasonable agreement with the resistivities reported in the literature (6, 7, 8). The actual resistivity may be less than that indicated, since surface roughness may increase the apparent film thickness measured with a profilometer on a step etched through the tungsten.

Stress

The stress was determined by measuring the wafer curvature before and after tungsten deposition with a Canon Model LSF-500 laser-scanning flatness tester (with no vacuum applied). The change in wafer curvature (i.e., the deformation resulting from the tungsten film deposition) increased approximately linearly with increasing tungsten thickness (Fig. 1), although there was significant scatter in the data. The stress caused the wafer to become concave upward, indicating that the stress in the tungsten film was tensile. Based on the linear increase of wafer deformation with increasing film thickness, the stress was calculated (9, 10) to be approximately 2×10^9 dyn/cm², in reasonable agreement with the value of 1.4×10^9 dyn/cm² expected from the difference in the linear coefficients of expansion of tungsten and silicon and the deposition temperature of 300°C. [The stress was calculated using values of 1.13×10^{12} and 3.4×10^{12} dyn/cm² for Young's modulus of silicon and tungsten, respectively (11), and 3×10^{-6} and $4.5 \times 10^{-6}/^\circ\text{C}$ for the corresponding linear coefficients of thermal expansion (11, 12).] Although the range of values reported for the coefficients used in the calculations makes the value of stress given here somewhat uncertain, the major portion of the stress probably arises from the difference

*Electrochemical Society Active Member.

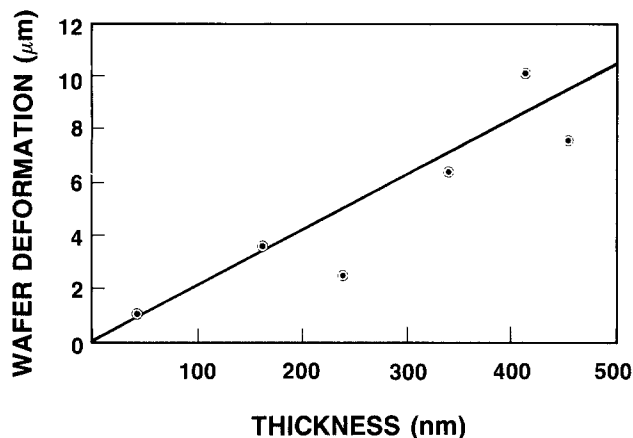


Fig. 1. Deformation of a 3 in. diam wafer as a function of tungsten film thickness.

in the thermal coefficients of expansion of tungsten and silicon.

The value found in this study is of the same sense, but markedly less in magnitude, than those reported by Green and Levy (8). While Green and Levy deposited tungsten on silicon, in the present study the films were deposited on a chromium nucleating layer so that the initial silicon reduction reaction was suppressed. This suggests that a significant contribution to the stress can arise from the initial reaction and little intrinsic stress is added during the hydrogen reduction reaction (13).

Surface Roughness

The surface roughness was observed under an optical microscope to increase with increasing film thickness (Fig. 2). Quantitative information about the surface roughness and its variation with film thickness was obtained by measuring the absolute sample reflectance over the 200-800 nm wavelength range with a Hewlett-Packard 8450A spectrophotometer.

To obtain the surface roughness from the reflectance data, the optical constants of tungsten over the wavelength range from 450 to 800 nm (14) were used to calculate the expected reflectivity R (assuming a

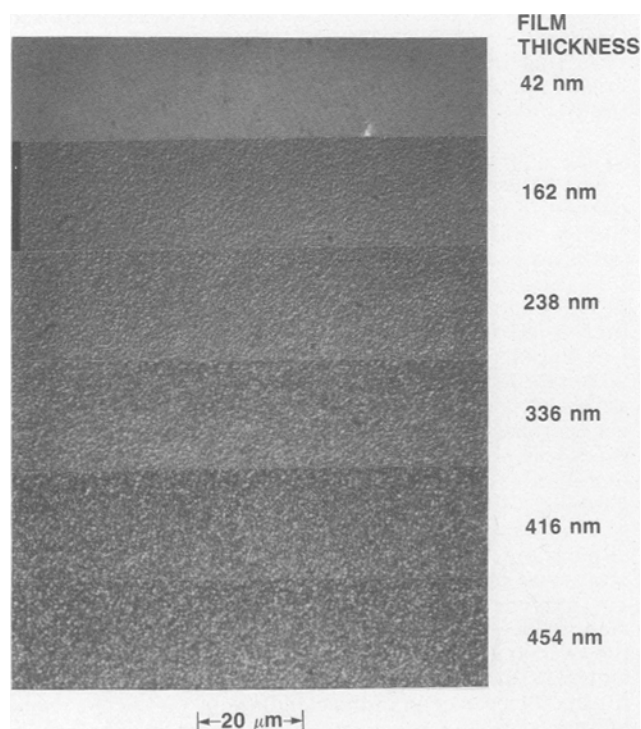


Fig. 2. Effect of tungsten film thickness on surface roughness; 300°C deposition temperature; Nomarski optical micrographs.

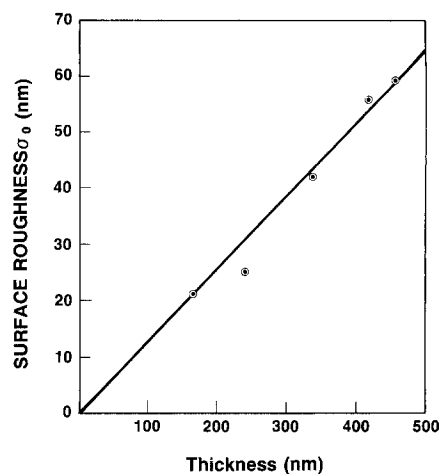


Fig. 3. Surface roughness as a function of tungsten film thickness

smooth, infinitely thick tungsten sample). The difference (on a log scale) between the calculated value and the observed reflectivity was taken as a measure of the surface roughness.

The surface roughness was then calculated from the formula (15)

$$\sigma_0 = 0.14 \lambda \sqrt{A - A_0}$$

where the measured quantity A is $-2 \log_{10} R$. The surface roughness calculated from the reflectivity is plotted as a function of film thickness in Fig. 3. It increases almost linearly with increasing thickness, consistent with the increasing surface roughness seen under the optical microscope, and appears to be about 12% of the film thickness. The surface roughness calculated from data at four different wavelengths within the range 472-622 nm agreed well, with a standard deviation of 3% or less, lending confidence to the technique used.

The surface roughness was also observed on samples deposited over the temperature range from 250° to 375°C using either chromium or bulk silicon to promote nucleation of the deposit. Figure 4 shows the measured signal $A = -2 \log_{10} R$ at $\lambda = 450$ nm as a function of film thickness for samples deposited at different temperatures. The deposition temperature is indicated for each sample. This figure shows that the surface roughness is dominated by thickness variations between samples and increases only slightly with increasing deposition temperature over this limited temperature range. No significant difference in surface roughness is apparent between the two different substrates.

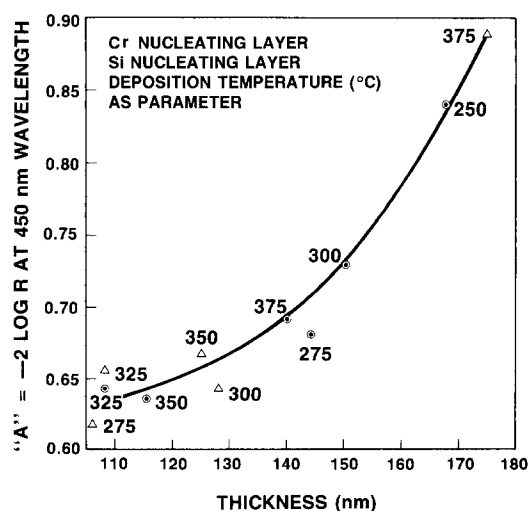


Fig. 4. Effect of deposition temperature on surface roughness, showing that film thickness is the more important variable.

Transmission Electron Microscopy

Grain size by plan-view TEM.—Plan-view transmission electron micrographs were prepared from CVD tungsten films with different thicknesses deposited at 300°C onto oxidized silicon wafers covered with a thin, sputtered chromium layer. The films were prepared for TEM analysis by chemically removing the silicon substrates from the backs of the tungsten films, but the tungsten films were not thinned. Therefore, the grain sizes are averages from the entire thickness of the tungsten film. (However, regions with many superposed small grains are less transparent, and the larger grains may be more readily seen.)

In plan-view, the grains appear to be approximately equi-axed with significant numbers of twins and dislocations within the grains (Fig. 5). The grain size is shown as a function of film thickness in Fig. 6 using the average and median of the grain sizes measured. The grain size increased as the film became thicker and was approximately equal to $\frac{3}{4}$ of the film thickness. The largest grains can have a diameter greater than the film thickness. The increase in grain size with increasing film thickness is consistent with the increase of surface roughness with thickness. In a similar study of CVD tungsten films (16), Learn and Foster also found that the grain size increased with increasing film thickness. However, the grain sizes they report are only about half those observed in the present study.

Transmission electron diffraction patterns did not indicate any strong preferred orientation. (The x-ray measurements to be discussed below are sensitive to smaller variations.) Significant numbers of crystal defects (twins and dislocations) were seen within some grains, but the incidence was less pronounced than in other materials [e.g., polysilicon (17)]. In the thinnest sample, some small ($<<10$ nm) nuclei were seen; these were probably from the chromium nucleating layer. These nuclei were not apparent on the thicker films but may be obscured by the larger amount of material through which the electron beam must penetrate.

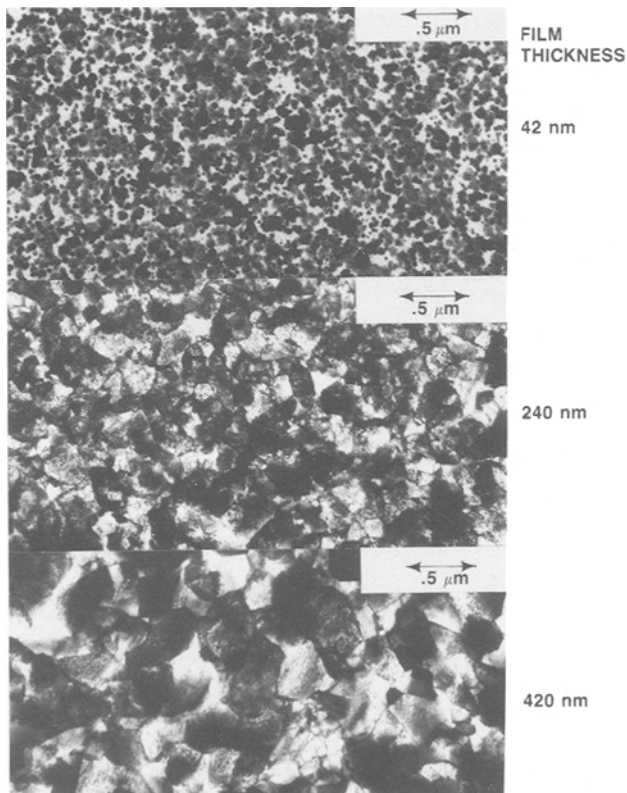


Fig. 5. Plan-view transmission electron micrographs of tungsten films 42, 240, and 420 nm thick.

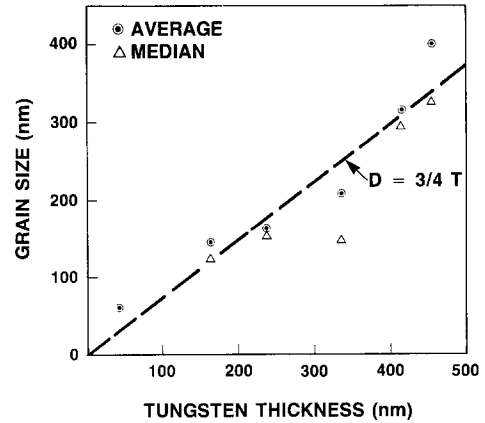


Fig. 6. Grain size as a function of tungsten film thickness

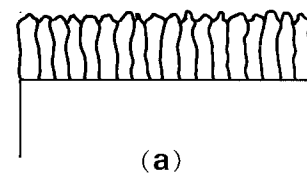
Cross-sectional TEM.—In previous studies of CVD tungsten films, a columnar grain structure developed as the film became thicker (18). A columnar structure could lead to deleterious electrical and chemical effects, such as resistivity anisotropy and rapid impurity diffusion along the grain boundaries through the thickness of the film, as seen in polysilicon (19). In one study, where the columnar grains were observed (18), the films were deposited at a much higher temperature (about 500°C) than used in the present study, and they were much thicker (about 0.65 cm).

To determine if a similar columnar structure (such as that shown schematically in Fig. 7a) develops under the deposition conditions used here, attempts were made to prepare cross-sectional samples for transmission electron microscopy. The thicker CVD tungsten films deposited on Cr nucleating layers were investigated. However, the markedly different sputtering and chemical etching rates of the CVD tungsten film and the silicon substrate made sample preparation difficult.

Within the limited area available for analysis, some grains were seen to extend completely through the 400 nm thickness of the samples. The grains were approximately equi-axed (as shown schematically in Fig. 7b) with their height only about twice their width. The tops of the grains were highly faceted. No obvious columnar structure was found. However, a columnar structure similar to that seen in the previous study could develop in very thick films. The present films may be much too thin for a columnar structure to develop, or the lower deposition temperature may inhibit formation of this structure.

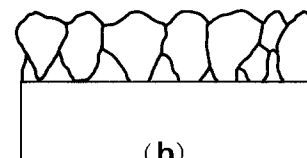
The information obtained from the cross-sectional TEM's is consistent with that from the other structural

COLUMNAR STRUCTURE



(a)

EQUI-AXED STRUCTURE



(b)

Fig. 7. Schematic cross-sectional views of (a) columnar and (b) equi-axed structures.

studies. The grains are approximately equi-axed, rather than columnar, and increase in size as the film becomes thicker. The larger grains lead to a rougher surface in the thicker films.

Preferred Orientation by X-Ray Analysis

The diffracted x-ray signal was measured as a function of the angle of the incident x-ray beam using a General Electric θ -2 θ x-ray diffractometer to provide a quantitative comparison of the relative prevalence of grains with normals in different low-index directions. Comparison of data from different samples showed how this texture varied as the deposition conditions were changed. To allow this comparison, all x-ray data were normalized by the powder-pattern intensities expected from a randomly oriented, infinitely thick, tungsten sample (20). The x-ray data were also corrected for film thickness variations from one sample to another (21) to remove the differences in x-ray signal strength arising from the differing amounts of tungsten intercepted in samples with different thicknesses. The resulting data are a measure of the relative prevalence of grains with their normals in the indicated direction (*i.e.*, the film "texture").

Effect of film thickness.—Considering films of varying thickness allowed the development of preferred orientation to be investigated as the film becomes thicker. Using a chromium nucleating layer removed the possibility of the structure being influenced by the initial reaction between WF_6 and silicon from the substrate.

Figure 8 shows that the (100) texture was dominant over the entire range of film thicknesses investigated. The relative importance of the (100) texture (after correcting for the film thickness) increased continuously with increasing thickness, indicating that the structural development is primarily dominated by the growth process, rather than by nucleation. The (100) texture did show a tendency to saturate in the thicker films. The increase in (100) texture with increasing film thickness correlates with the increase in grain size seen by TEM as the film becomes thicker, implying that the (100)-oriented grains grow at the expense of those with other orientations.

Most of the other textures remained constant with increasing film thickness after an initial increase for films less than 170 nm thick. The weak x-ray signals observed in the thinnest film may reflect limits on the sensitivity of the x-ray equipment, or they may be related to the structure in the first parts of the film deposited, which contains small grains that may have many different orientations. The (310), (110), and (211) textures appeared to be of similar intensity and were all much less important than was the (100) texture. The (310) texture increased with increasing film thickness, while the other

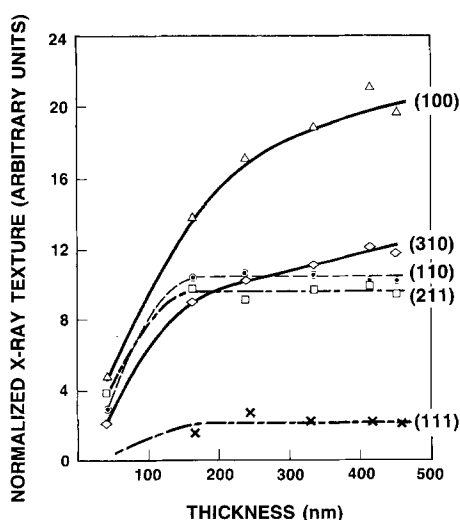


Fig. 8. Normalized x-ray texture as a function of film thickness; 300°C deposition temperature.

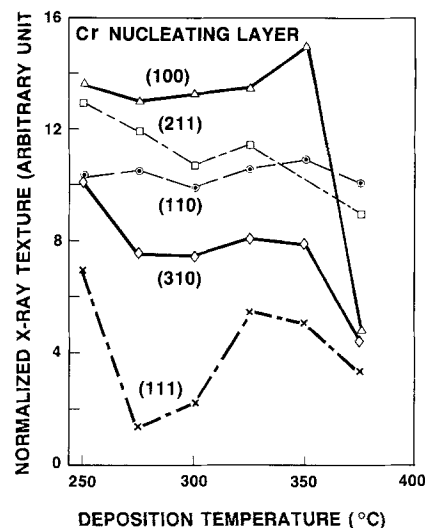


Fig. 9. Normalized x-ray texture as a function of deposition temperature.

secondary textures did not. The (111) texture was much weaker and also tended to remain constant after an initial increase for the thinnest films.

Effect of deposition temperature.—CVD tungsten films were deposited over the deposition temperature range from 250° to 375°C with thicknesses generally between 100 and 150 nm. Films were deposited on both bare silicon wafers and on thin chromium nucleating layers on oxidized silicon wafers. The normalized x-ray data obtained from tungsten films deposited on Cr nucleating layers are shown in Fig. 9.

Between 250° and 325°C, the most important textures did not vary significantly with temperature. The (111) texture appeared to be quite large in the 250°C sample. This film was somewhat thicker than the others, but Fig. 8 suggests that this thickness difference should not have greatly influenced the results. Above 300°C, the (111) texture increased also, but it was not dominant in any case. At 375°C, the (100) texture appeared to decrease dramatically, with the (110) and (211) textures becoming more important.

Similar trends in the preferred orientation were seen in tungsten films deposited on bulk silicon wafers as the deposition temperature was changed, again suggesting that the crystal structure is dominated by the growth mechanisms, rather than by the initial nucleation.

This investigation of the temperature variation of the structure shows that, near the standard operating temperature of 300°C, the structure is not a sensitive function of the deposition temperature, making temperature control less critical near 300°C than in other temperature ranges to obtain a reproducible film structure. (The deposition rate is still a sensitive function of temperature, however.)

Effect of nucleating layer.—To obtain more direct information about the effect of the underlying layers on the growth and development of the structure in CVD tungsten films, films were deposited on several different nucleating layers (Table I).

The relative amounts of the low index crystal orientations are shown in Fig. 10 for all except the sputtered

Table I. Substrates used for CVD tungsten deposition

Oxidized Si wafer + thin sputtered Cr film (nominally 8 nm thick)
Oxidized Si wafer + thin sputtered Si film (nominally 8 nm thick)
Oxidized Si wafer + 560 nm LPCVD amorphous silicon
Oxidized Si wafer + 410 nm undoped LPCVD polysilicon
Oxidized Si wafer + 370 n ⁺ LPCVD polysilicon
Oxidized Si wafer + 100 nm sputtered W
n ⁻ bulk Si wafer
n ⁺ bulk Si wafer (doped using POCl ₃)

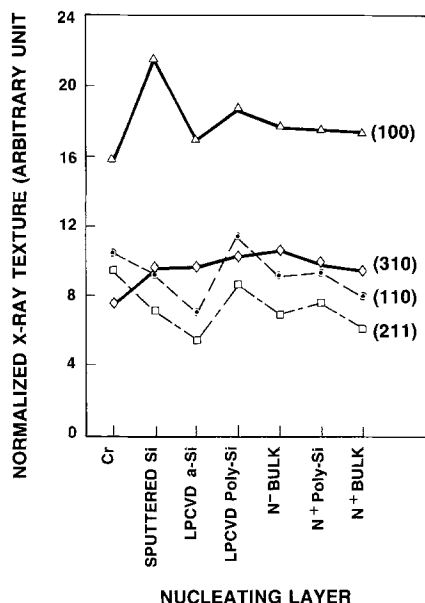


Fig. 10. Effect of nucleating layer on x-ray texture

tungsten nucleating layer. Excluding the latter, the observed orientations did not differ significantly except for the sputtered silicon nucleating layer. The (100) texture was dominant in all cases (again excluding the sputtered tungsten). The small differences seen for most of the nucleating layers again suggests that the growth process dominates the development of structure in the films; that is, the texture is primarily a growth texture, rather than a nucleation texture.

The effect of the thick sputtered tungsten nucleating layer appeared to be more significant. In this case, the (110) texture was dominant, instead of the (100) texture. The (211) texture was second, followed by the (310) texture. The (100) texture was less significant than the other three. Although the sputtered tungsten nucleating layer appeared to suppress the (100) texture, the nucleating layer in this case was almost as thick as the CVD tungsten layer, so the x-ray signal sampled the texture in both the sputtered and CVD tungsten layers. In addition to contributing to the measured signal, the structure in the fine-grain sputtered tungsten should influence the structure in the subsequently deposited CVD tungsten film. The other nucleating layers may have structures that are not commensurate with the tungsten structure and, therefore, may not influence the structure of the CVD tungsten as significantly.

Summary

The properties of CVD tungsten films have been examined over a range of deposition conditions and with varying nucleating layers. When the tungsten is deposited on a chromium nucleating layer on an oxidized silicon wafer, the stress does not depend strongly on film thickness and is close to that expected from the different coefficients of thermal expansion of tungsten and silicon. The surface roughness increases almost linearly with increasing film thickness. The grain size increases with

increasing film thickness, with the diameters of the largest grains being comparable to the film thickness. The (100) texture is dominant near the normal deposition temperature of 300°C for different film thicknesses and nucleating layers, but the dominant orientation changes at higher deposition temperatures. The structure develops as the film grows, rather than being determined by the nucleation.

The controllable film properties should allow reproducible deposition of LPCVD tungsten films for a variety of integrated circuit applications.

Acknowledgment

The authors would like to thank H. Birenbaum, J. Turner, R. Smith, D. Hayes, and M. Juanitas for assistance with film deposition and evaluation, and D. Ilic and S. Y. Chiang for encouragement during this study.

Manuscript submitted Feb. 21, 1986; revised manuscript received May 19, 1986.

Hewlett-Packard Laboratories assisted in meeting the publication costs of this article.

REFERENCES

1. N. E. Miller and I. Beinglass, *Solid State Technol.*, **25**, 85 (December 1982).
2. K. C. Saraswat, in "VLSI Science and Technology," W. M. Bullis and S. Broydo, Editors, p. 409, The Electrochemical Society Softbound Proceedings Series, Pennington, NJ (1984).
3. T. I. Kamins, S. S. Laderman, D. J. Coulman, and J. E. Turner, *This Journal*, **133**, 1438 (1986).
4. D. R. Bradbury and T. I. Kamins, *ibid.*, **133**, 1214 (1986).
5. E. K. Broadbent and C. L. Ramiller, *ibid.*, **131**, 1427 (1984).
6. C. M. Melliar-Smith, A. C. Adams, R. H. Kaiser, and R. A. Kushner, *ibid.*, **121**, 298 (1974).
7. Y. Pauleau, *Thin Solid Films*, **122**, 243 (1984).
8. M. L. Green and R. A. Levy, *This Journal*, **132**, 1243 (1985).
9. D. S. Campbell, in "Basic Problems in Thin Film Physics," R. Niedermayer and H. Mayer, Editors, p. 227, Vandenhoeck and Ruprecht, Göttingen (1966).
10. K. Kinoshita, *Thin Solid Films*, **12**, 17 (1972).
11. "American Institute of Physics Handbook," 3rd ed., D. E. Gray, Editor, pp. 2-67, 4-129, 4-131, McGraw-Hill, New York (1972).
12. "Tables for Applied Engineering and Science," Chemical Rubber Co. (1970).
13. D. Paine, Stanford University, Private communication.
14. "American Institute of Physics Handbook," 3rd ed., D. E. Gray, Editor, pp. 6-153, McGraw-Hill, New York (1972).
15. K. L. Chiang, C. J. Dell'Oca, and F. N. Schwettmann, *This Journal*, **126**, 2267 (1979).
16. A. J. Learn and D. W. Foster, *J. Appl. Phys.*, **58**, 2001 (1985).
17. T. I. Kamins and T. R. Cass, *Thin Solid Films*, **16**, 147 (1973).
18. J. M. Blocher, Jr., in "Deposition Technologies for Films and Coatings," R. F. Bunshah, Editor, p. 358, Noyes Publications, Park Ridge, NJ (1982).
19. T. I. Kamins, J. Manoliu, and R. N. Tucker, *J. Appl. Phys.*, **43**, 83 (1972).
20. "X-Ray Powder Data File," J. V. Smith, Editor, American Society for Testing and Materials, Philadelphia (1960).
21. B. D. Cullity, "Elements of X-Ray Diffraction," p. 270, Addison-Wesley, Reading, MA (1956).